UNIVERSITÉ
DE GENÈVE
FACULTÉ DES SCIENCES

DQMP
http://supra.unige.ch

Superconductivity and its applications

Lecture 10

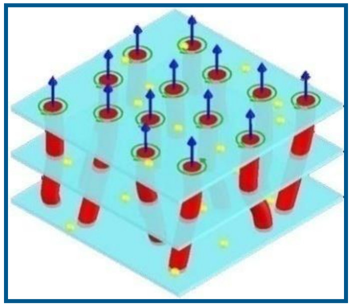

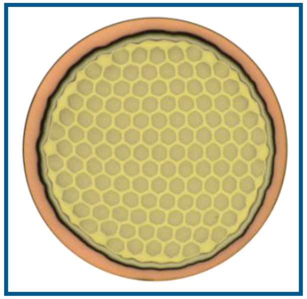

Carmine SENATORE

Group of Applied Superconductivity
Department of Quantum Matter Physics
University of Geneva, Switzerland

Previously, in lecture 9
HTS materials for applications

Copper oxides with highly anisotropic structures, texturing (grain orientation) is required in technical superconductors

	T_c [K]	texture	
Bi2223	110	c-axis	
Bi2212	91	c-axis (radial)	
Y123	92	biaxial	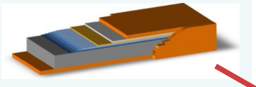

Produced by Powder-In-Tube method
Ag matrix material
Tape geometry to achieve c-axis texturing
I_c depends on the magnetic field orientation

Produced by Powder-In-Tube method
Ag matrix material
Round wire, spontaneous radial texturing of the c-axis
Isotropic properties of I_c

Coated conductors
Y123 layer deposited on a metallic substrate
Texturing along c and in the ab plane
I_c depends on the magnetic field orientation

Previously, in lecture 9

Superconducting magnets, field shapes and winding configurations

Solenoids (NMR, MRI and laboratory magnets)

$$B_0 = JaF(\alpha,\beta) \quad \text{where} \quad J = \frac{NI}{2l(b-a)}$$

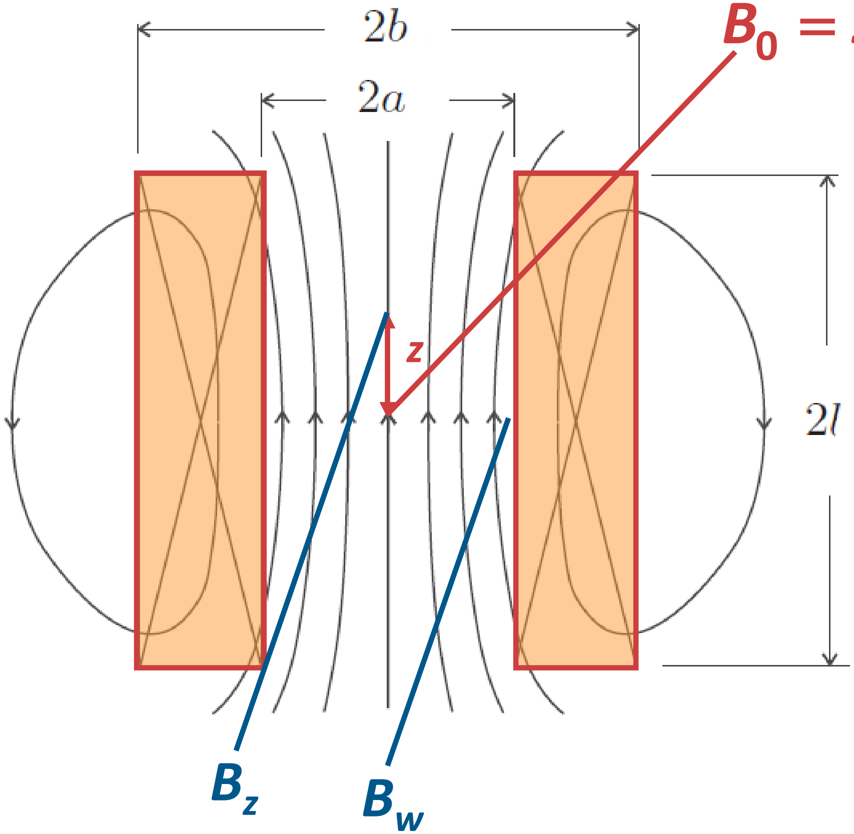

$$F(\alpha,\beta) = \mu_0 \beta \ln\left[\frac{\alpha + \sqrt{\alpha^2+\beta^2}}{1+\sqrt{1+\beta^2}}\right]$$

$$\alpha = \frac{b}{a} \qquad \beta = \frac{l}{a}$$

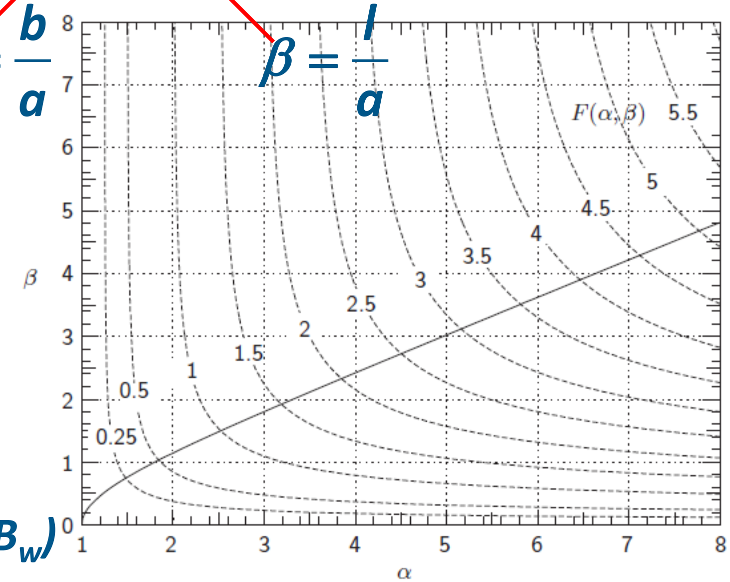

α and β have an influence on the field uniformity (B_z and B_w)

Previously, in lecture 9

Notched solenoids and homogeneity along z

$$B_z = B_0\left[1 + E_2\left(\frac{z}{a}\right)^2 + E_4\left(\frac{z}{a}\right)^4 + E_6\left(\frac{z}{a}\right)^6 + \dots\right]$$

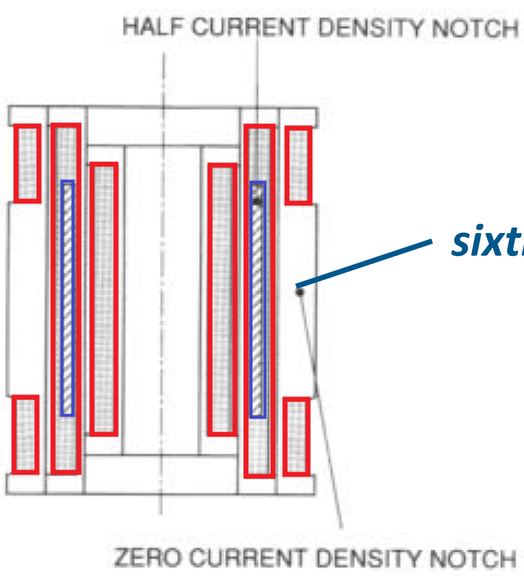

sixth order $E_2 = E_4 = 0$

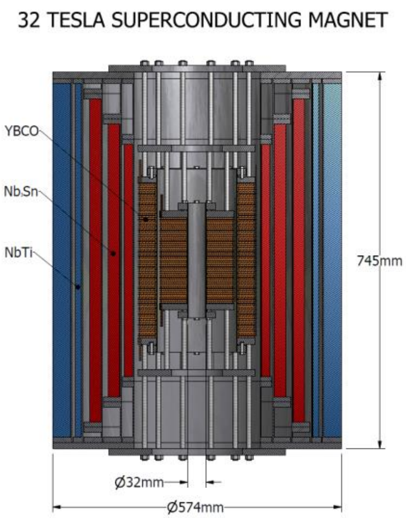

General guidelines for magnet design

Subdivide the winding into a number of concentric sections to improve the efficiency of superconductor utilization

All sections take the same current, but each section has its own J, α and β

Each section operates at the maximum current density allowed by the local field level

Transverse fields: accelerator magnets

Sketch of coils to generate transverse fields

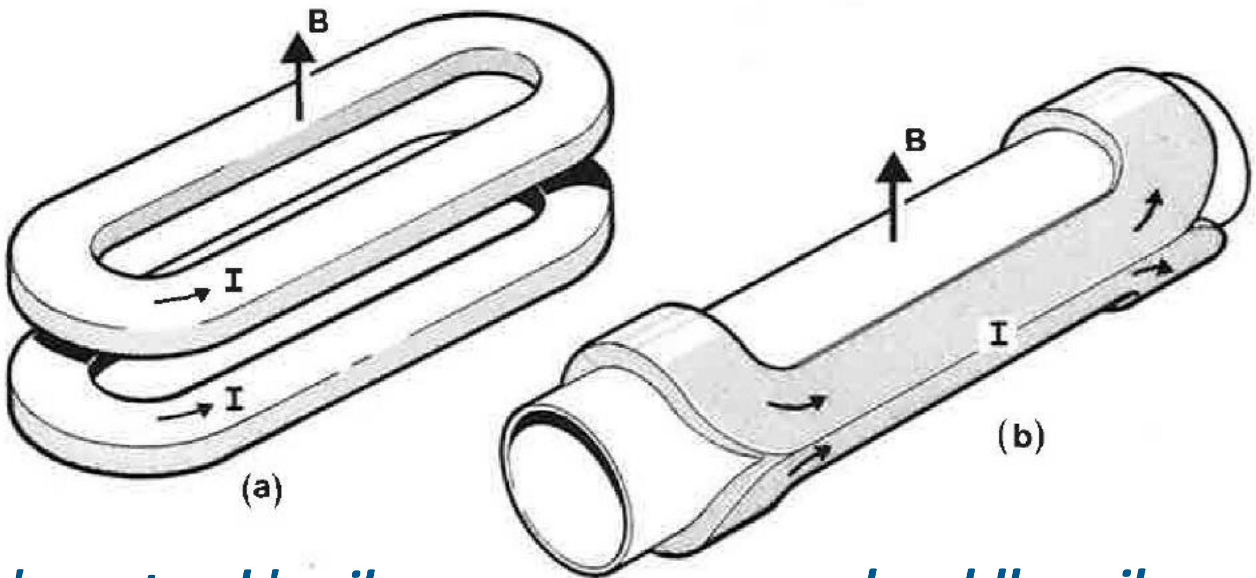

flat 'race track' coils

curved saddle coils

Transverse fields: accelerator magnets

Bending the beam

Uniform field (dipole)

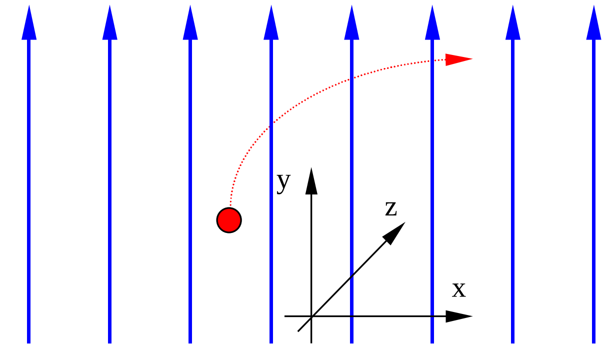

Focusing the beam

Gradient field (quadrupole)

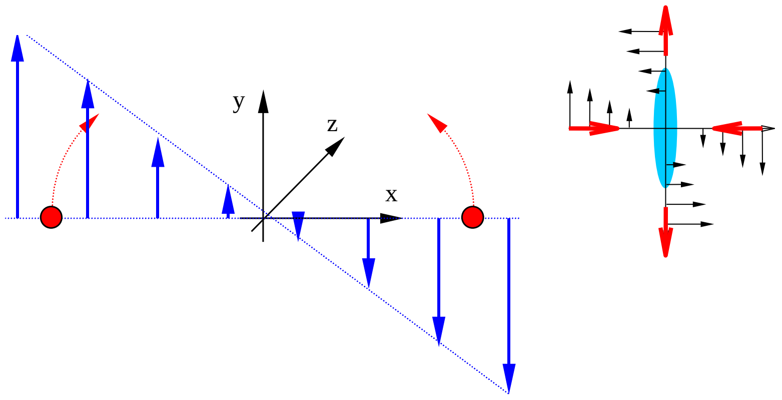

Infinite cylinders carrying uniform J

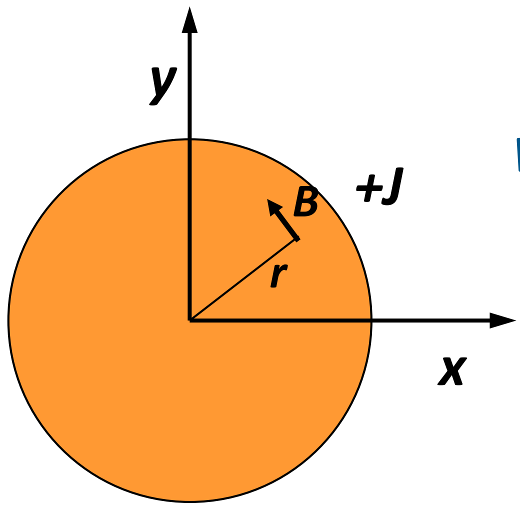

Within a cylinder carrying uniform J, the field is

$$B = \mu_0 \frac{Jr}{2}$$

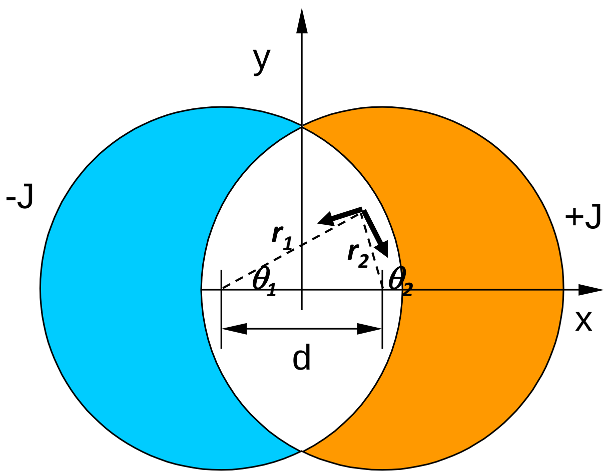

Two cylinders with their centres spaced apart by d and carrying uniform J but oppositely directed

$$B_y = \frac{\mu_0 J}{2}\left[-r_1 \cos\theta_1 + r_2 \cos\theta_2\right] = -\mu_0 \frac{Jd}{2}$$

$$B_x = \frac{\mu_0 J}{2}\left[r_1 \sin\theta_1 - r_2 \sin\theta_2\right] = 0$$

B_y is uniform over the whole aperture

Perfect dipole field

Multipole magnets

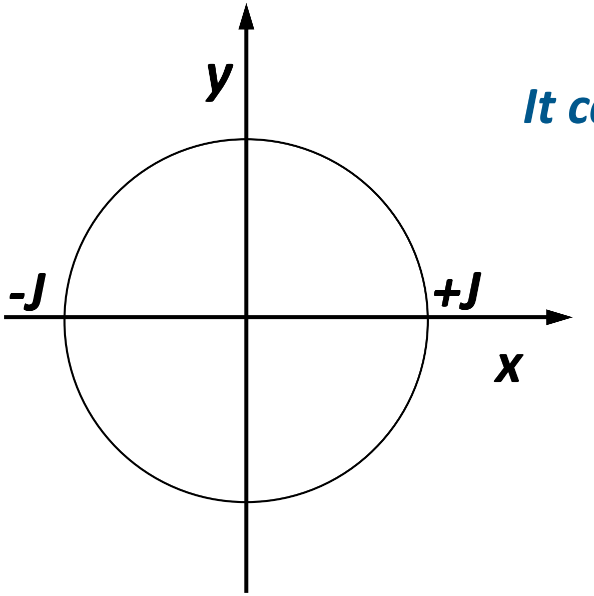

It can be demonstrated that:

A cylindrical current sheet, infinite along z, carrying a ***cosθ current*** *distribution generates a* ***perfect dipole field***

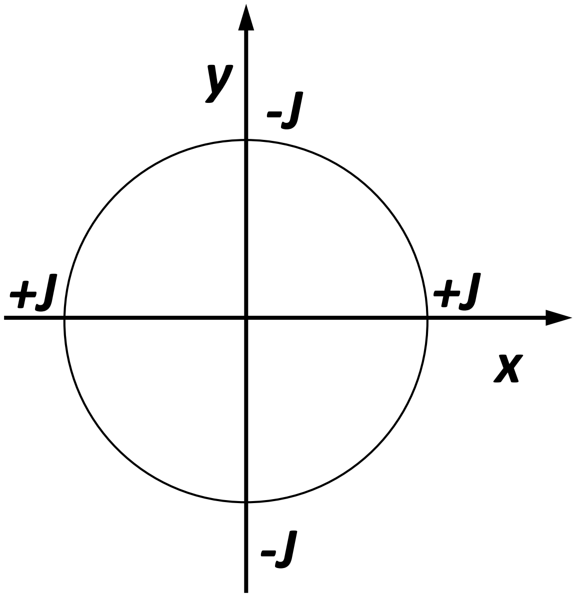

A cylindrical current sheet, infinite along z, carrying a ***cos2θ current*** *distribution generates a* ***perfect quadrupole field***

Intersecting ellipses carrying uniform J

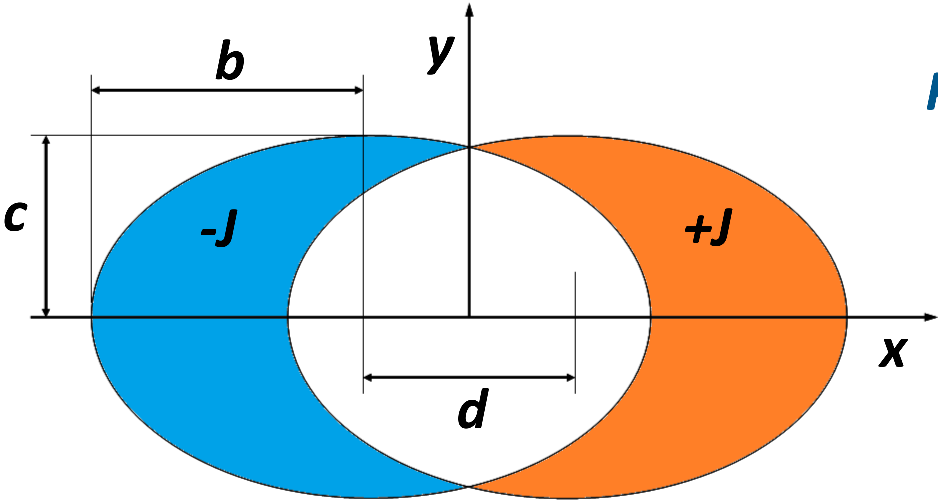

Perfect dipole

$$B_y = -\mu_0 \frac{Jdc}{(b+c)}$$

$$B_x = 0$$

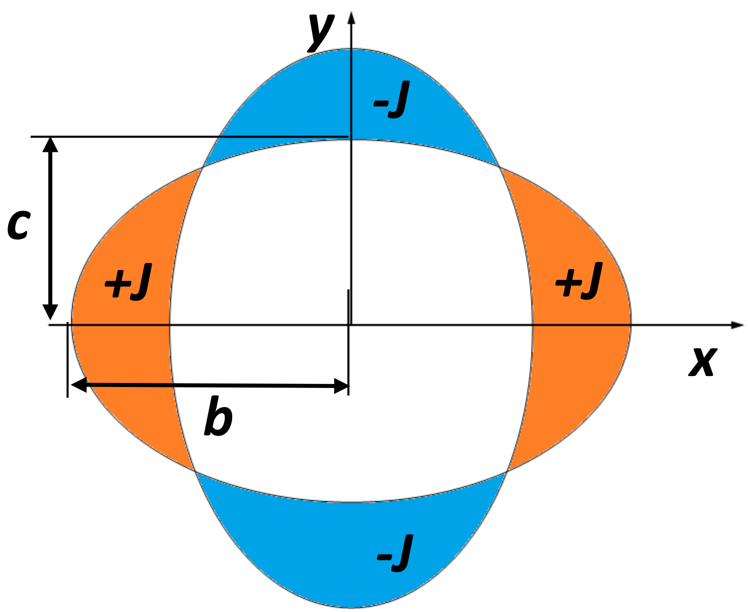

Perfect quadrupole

$$B_y = \frac{\mu_0 J(b-c)}{b+c} y$$

$$B_x = \frac{\mu_0 J(b-c)}{b+c} x$$

Uniform gradient $g = \dfrac{\mu_0 J(b-c)}{b+c}$

Real coil configurations for multipole magnets

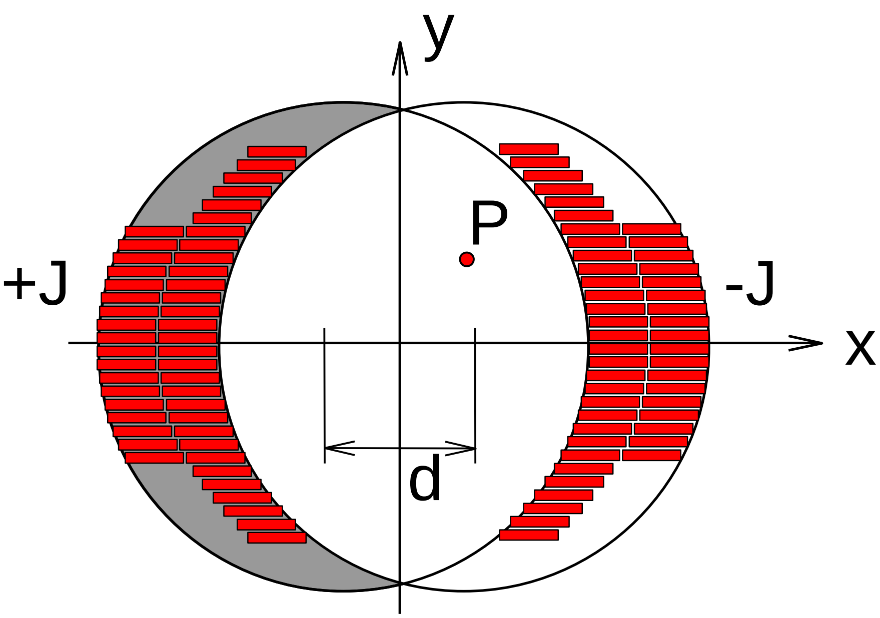

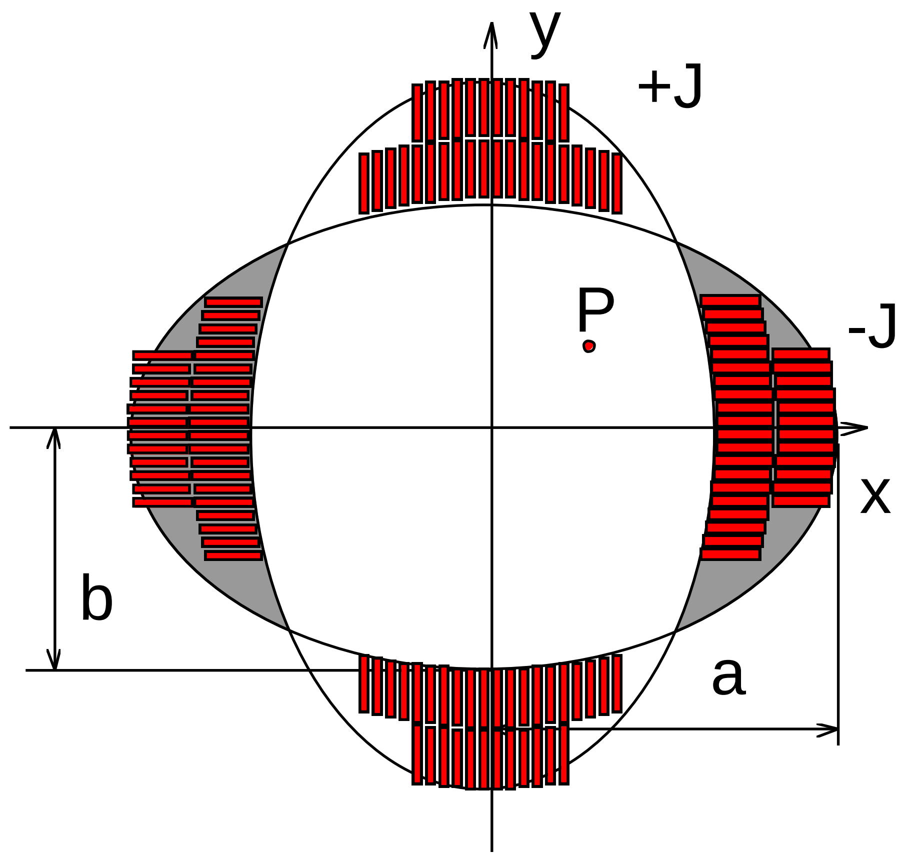

Approximation for the ideal dipole current distribution

Approximation for the ideal quadrupole current distribution

Harmonic generation in real coils

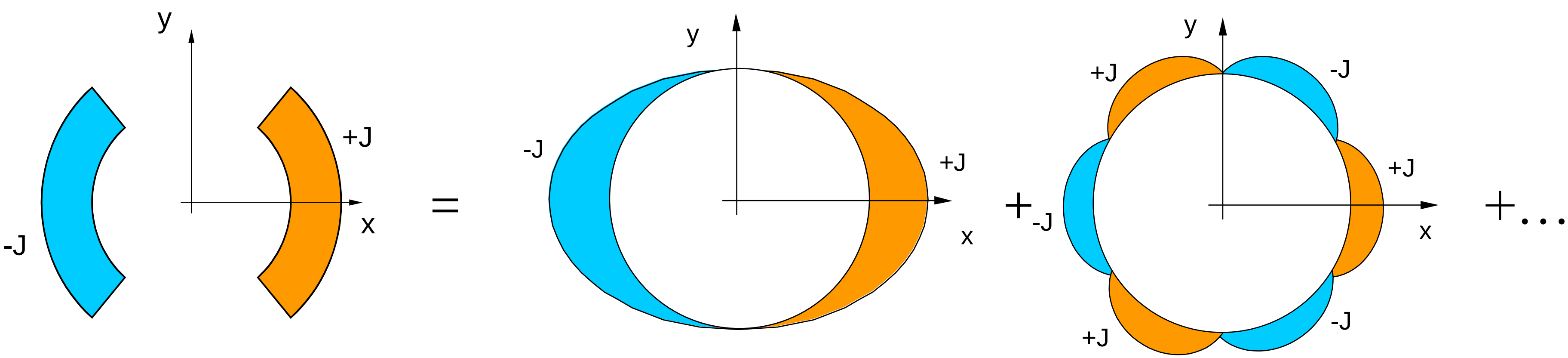

Uniform current shell = *cosθ current* + *cos3θ current* + ...

Magnetic field = *dipole field* + *sextupole term* + ...

LHC dipoles

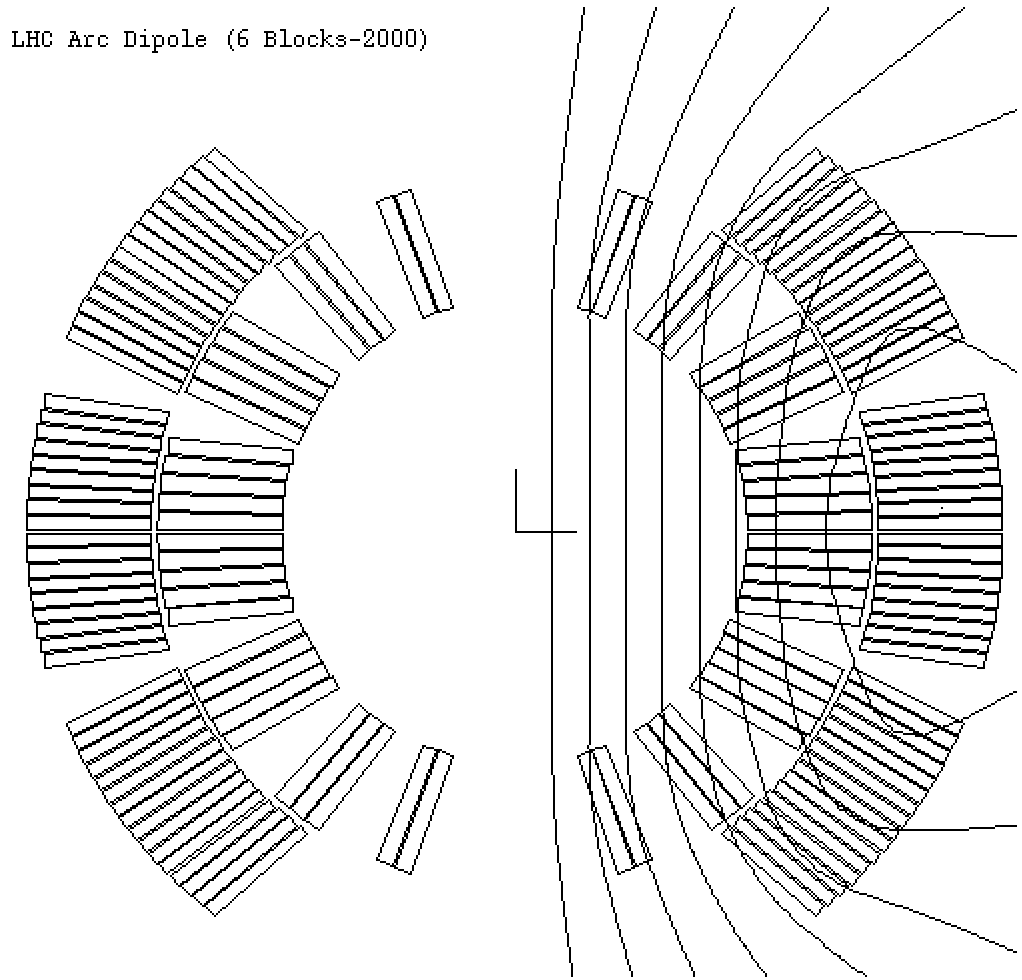

LHC quadrupoles

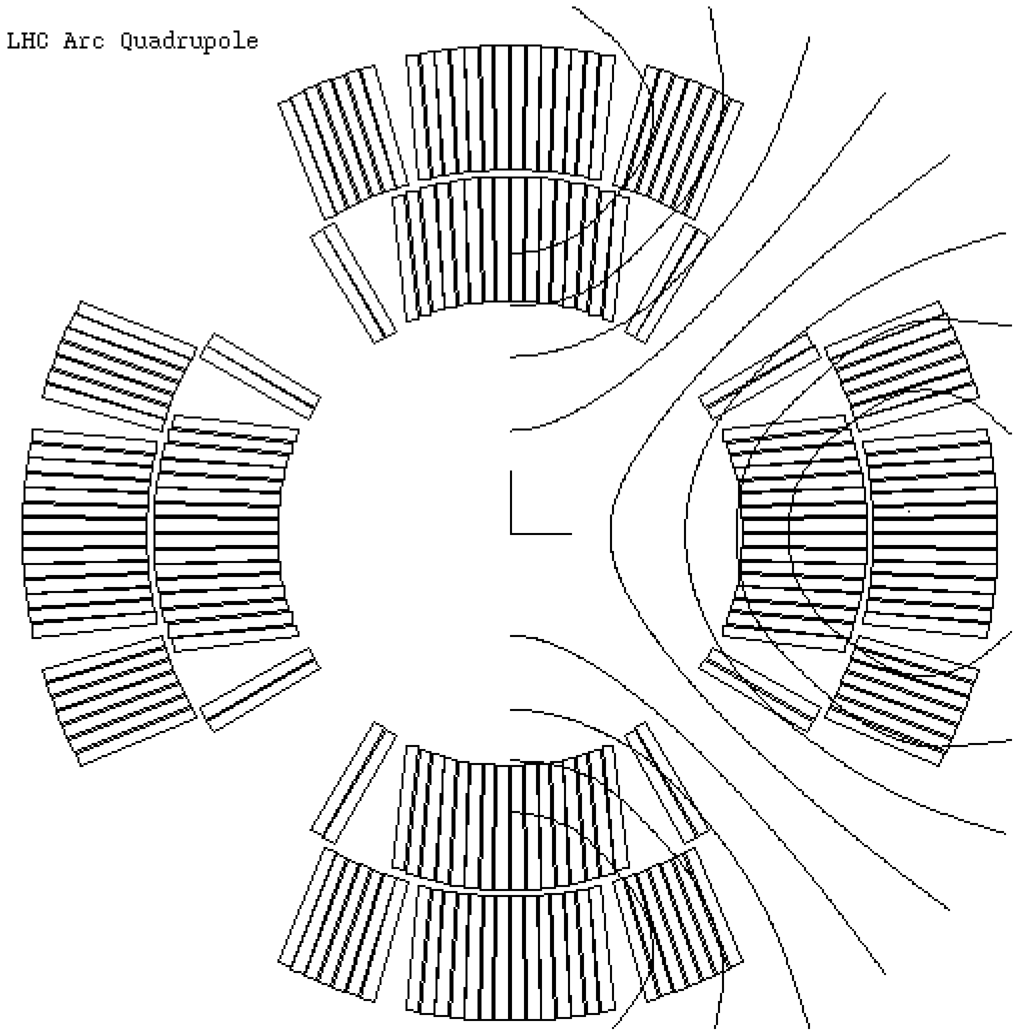

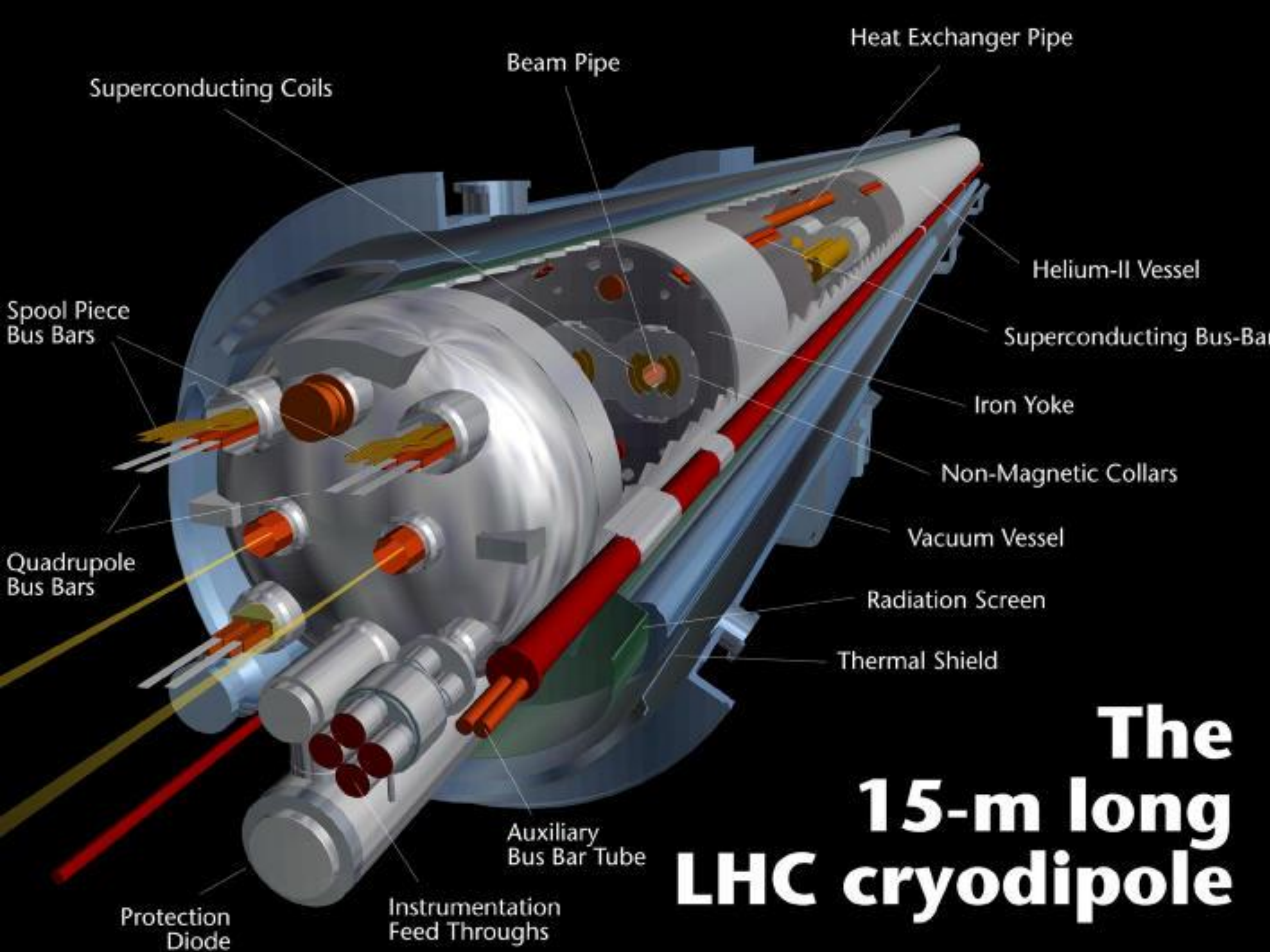
Heat Exchanger Pipe
Beam Pipe
Superconducting Coils
Helium-II Vessel
Spool Piece
Bus Bars
Superconducting Bus-Ba
Iron Yoke
Non-Magnetic Collars
Vacuum Vessel
Quadrupole
Bus Bars
Radiation Screen
Thermal Shield
Auxiliary
Bus Bar Tube
Instrumentation
Feed Throughs
Protection
Diode
The
15-m long
LHC cryodipole

Toroidal fields

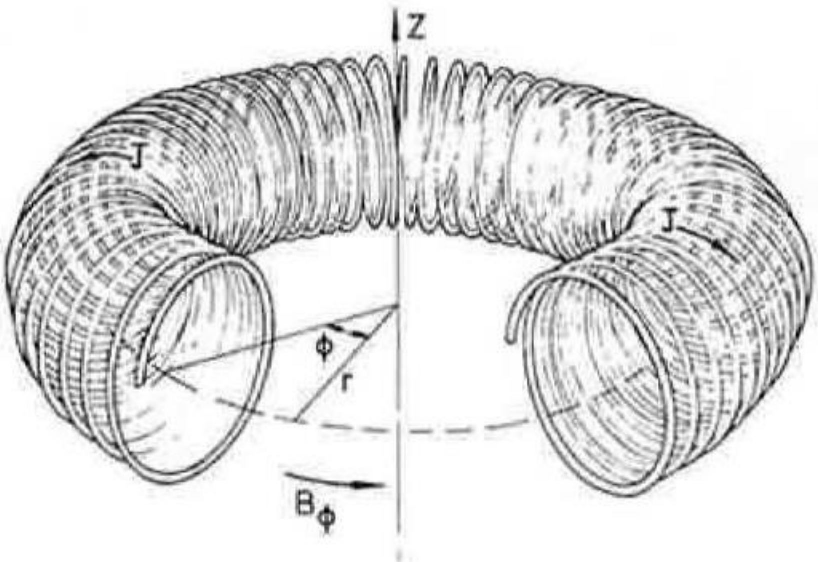

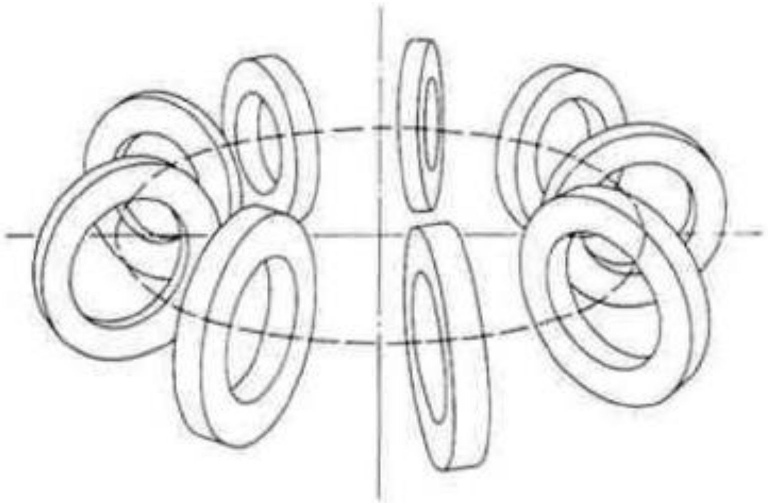

In a 'perfect' torus the distribution of current density is perfectly uniform in the ϕ direction

No field in the r- or z-directions

By applying Ampere's law

$$\int B_\varphi r d\varphi = B_\varphi 2\pi r = \mu_0 NI$$

$$\boxed{B_\varphi = \frac{\mu_0 NI}{2\pi r}}$$

A practical torus is constructed from a number of discrete circular coils

Toroidal fields: fusion magnets

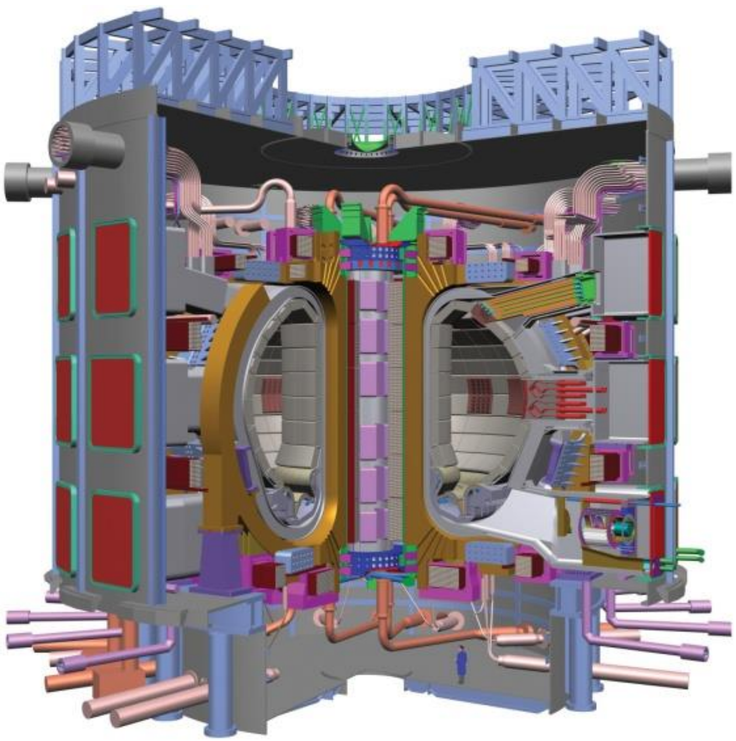

ITER Reactor

Toroidal windings produce fields in which the magnetic lines of force close up on themselves

It is difficult for charged particles to diffuse in directions perpendicular to the magnetic field lines

Closed-line configurations provide good confinement fields for the hot ionized plasmas which are needed to produce controlled thermonuclear fusion

Introduction to Forces and Stresses in a Magnet

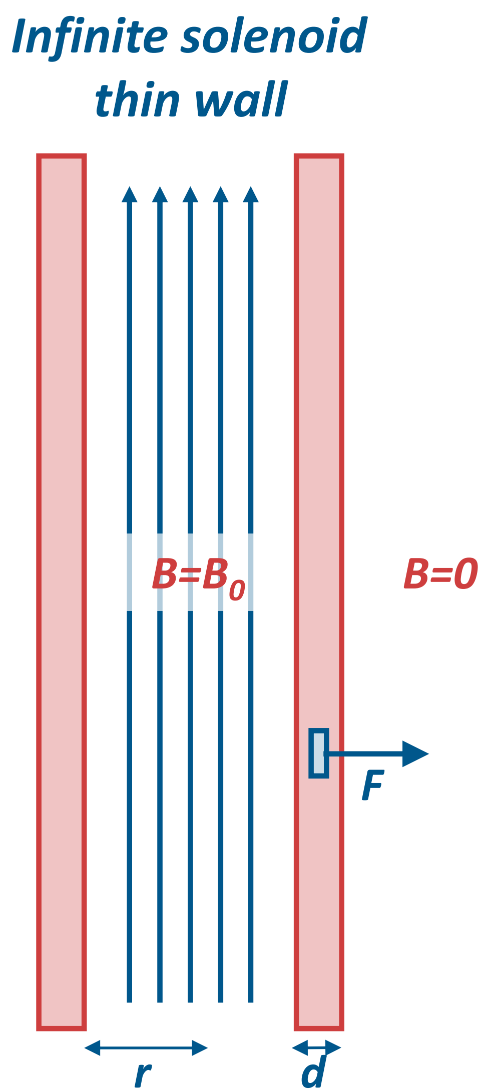

The magnetic field is $B_0 = \mu_0 J d$

The expression of the magnetic force density (per unit of volume) is

$$f = J \times B$$

The average field in the winding is $\dfrac{B_0}{2}$

The (radial) force on a winding volume element is

$$\Delta F = J \frac{B_0}{2} \Delta v = J \frac{B_0}{2} r \Delta\theta \, \Delta z \, d = \frac{B_0{}^2}{2\mu_0} r \Delta\theta \, \Delta z$$

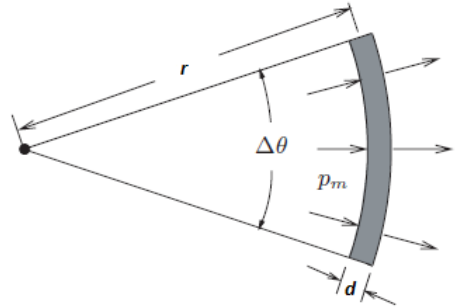

$$= \frac{B_0{}^2}{2\mu_0} \Delta s = p_m \Delta s$$

$$p_m(B_0 = 10T) = 400 \; bar$$

Hoop stress in a ring

A ring carrying a current I in a field B

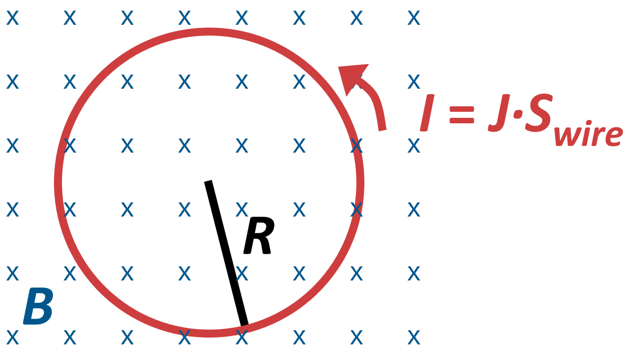

The total radial magnetic force on the ring is

$$F_r = \int_{loop} dv f = \int dv J \times B$$

$$= 2\pi \; R \; I \; B$$

Hoop stress in a ring

A ring carrying a current I in a field B

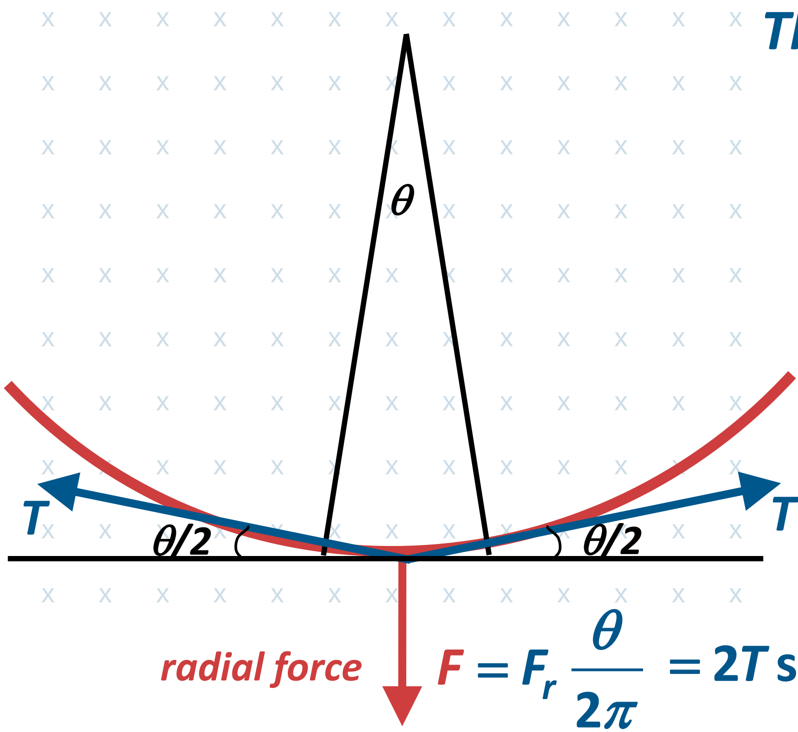

The total radial magnetic force on the ring is

$$F_r = \int_{loop} dv f = \int dv J \times B$$

$$= 2\pi \; R \; I \; B$$

A tension is developed within the ring

$$F = F_r \frac{\theta}{2\pi} = 2T \sin\frac{\theta}{2} \approx 2T\frac{\theta}{2} = T\theta \quad \Rightarrow T = \frac{F_r}{2\pi} = R \; I \; B$$

The so-called "hoop stress" on the wire is $\sigma_\theta = \dfrac{T}{S_{wire}} = R \; J \; B$

Hoop stress levels above 100 MPa are common, the NHMFL 32 T magnet operates at 400 MPa

Electromagnetic stresses in a finite solenoid

In a winding adjacent turns will press on each other and develop a radial stress σ_r which modifies the hoop stress σ_θ

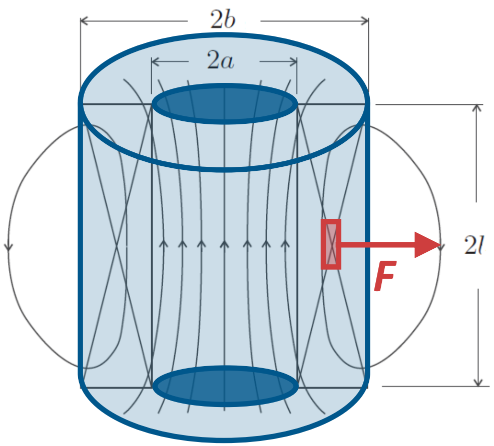

Considering the solenoid as a continuous uniform medium, from the Hooke's law

$$\sigma_r = \frac{E}{1-\nu^2}\left(\frac{du}{dr} + \nu\frac{u}{r}\right) \quad \text{and} \quad \sigma_\theta = \frac{E}{1-\nu^2}\left(\frac{u}{r} + \nu\frac{du}{dr}\right)$$

where u is the local displacement in the radial direction, E is the Young's modulus and ν is the Poisson's ratio

The condition for equilibrium between radial stress σ_r, hoop stress σ_θ and body force BJr is given by the equation

$$\frac{1}{r}\frac{d}{dr}\left(r\frac{du}{dr}\right) - \frac{u}{r^2} = \frac{1-\nu^2}{E}BJ$$

Electromagnetic stresses in a finite solenoid

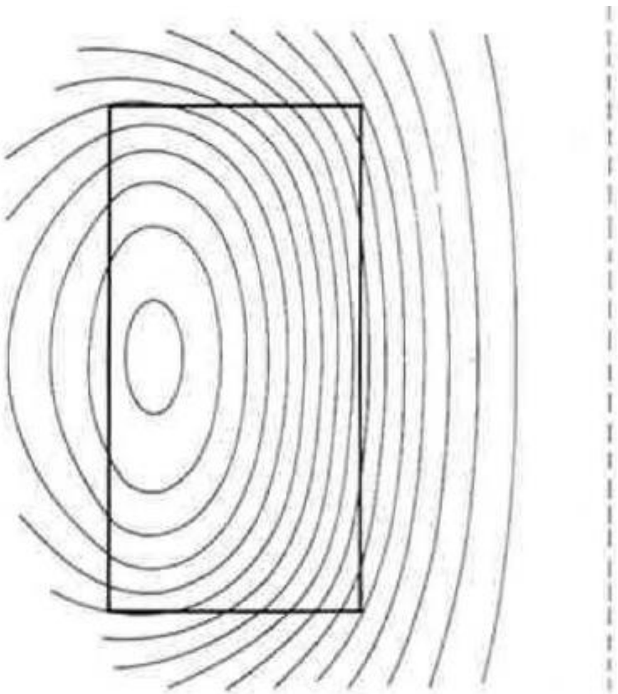

magnetic lines of force

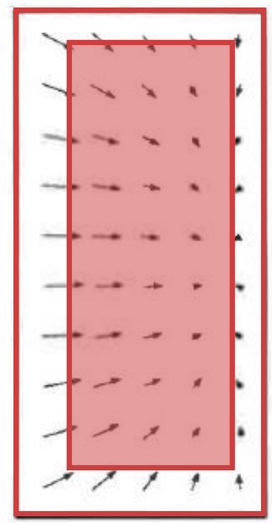

vectors of electromagnetic force per unit volume

$$p = \frac{B_0^{\,2}}{2\mu_0}$$

$$\sigma'_\theta = BJr$$

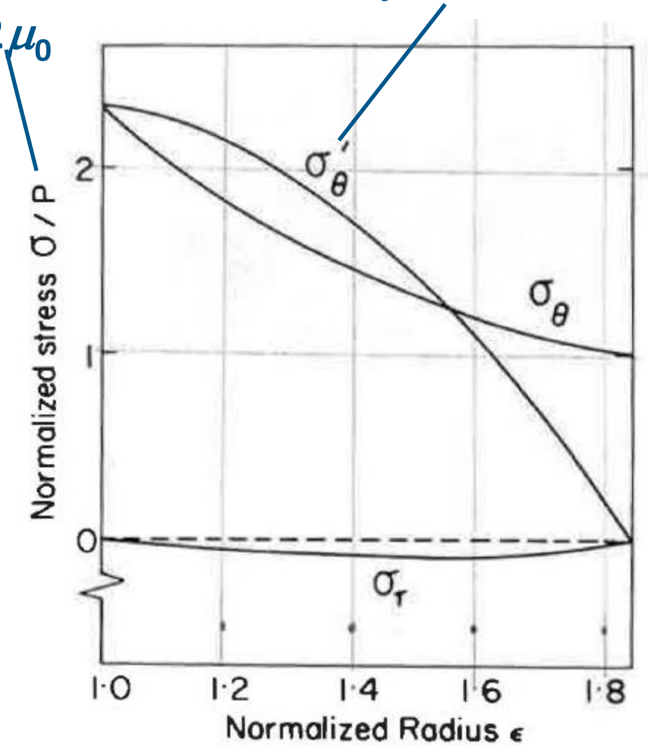

$$\varepsilon = \frac{r}{\text{bore radius}}$$

Example: for B_0 of the order of 10 T, on the winding σ_θ of > 200 MPa (> 2000 bar)

Electromagnetic stresses in an accelerator dipole

$$p = \frac{B_0^2}{2\mu_0}$$

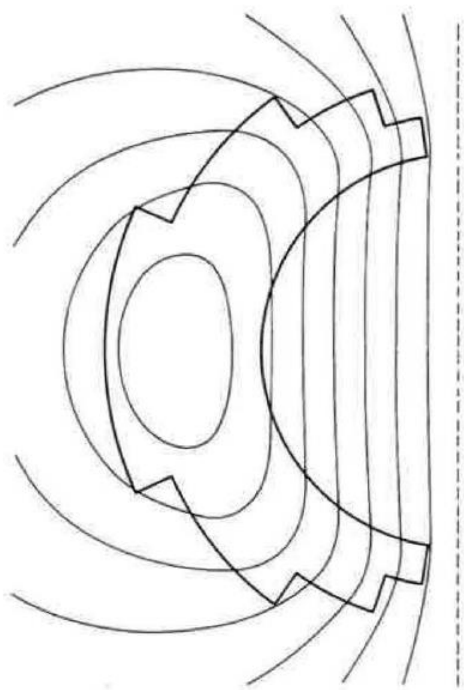

magnetic lines of force

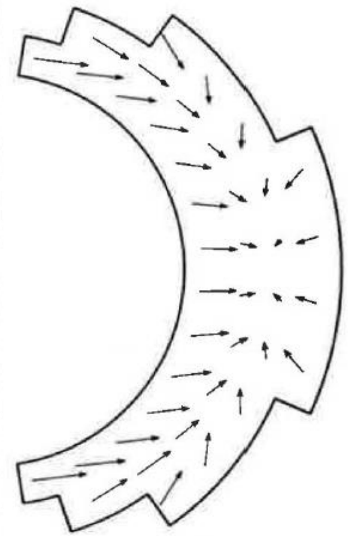

vectors of electromagnetic force per unit volume

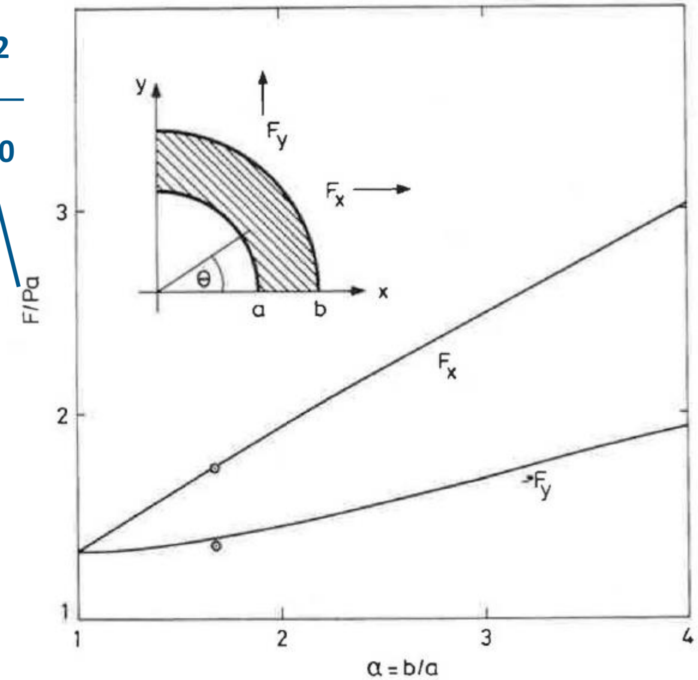

For B_0=6T and (a+b)/2=100 mm

F_x=200 tons/m

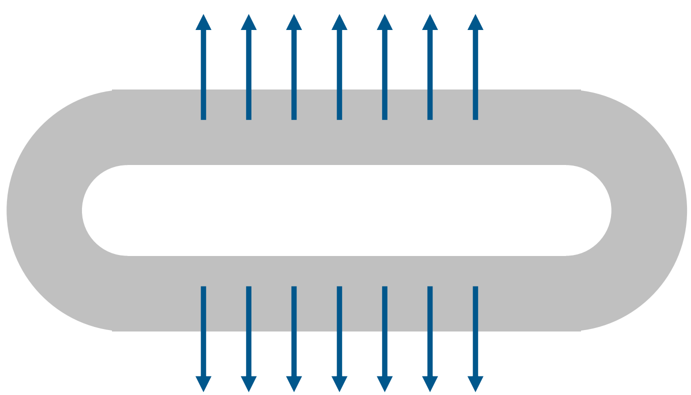

In straight-sided coils such as dipoles and quadrupoles the conductor is unable to support the magnetic forces in tension

How to make the dipole able to sustain the stress

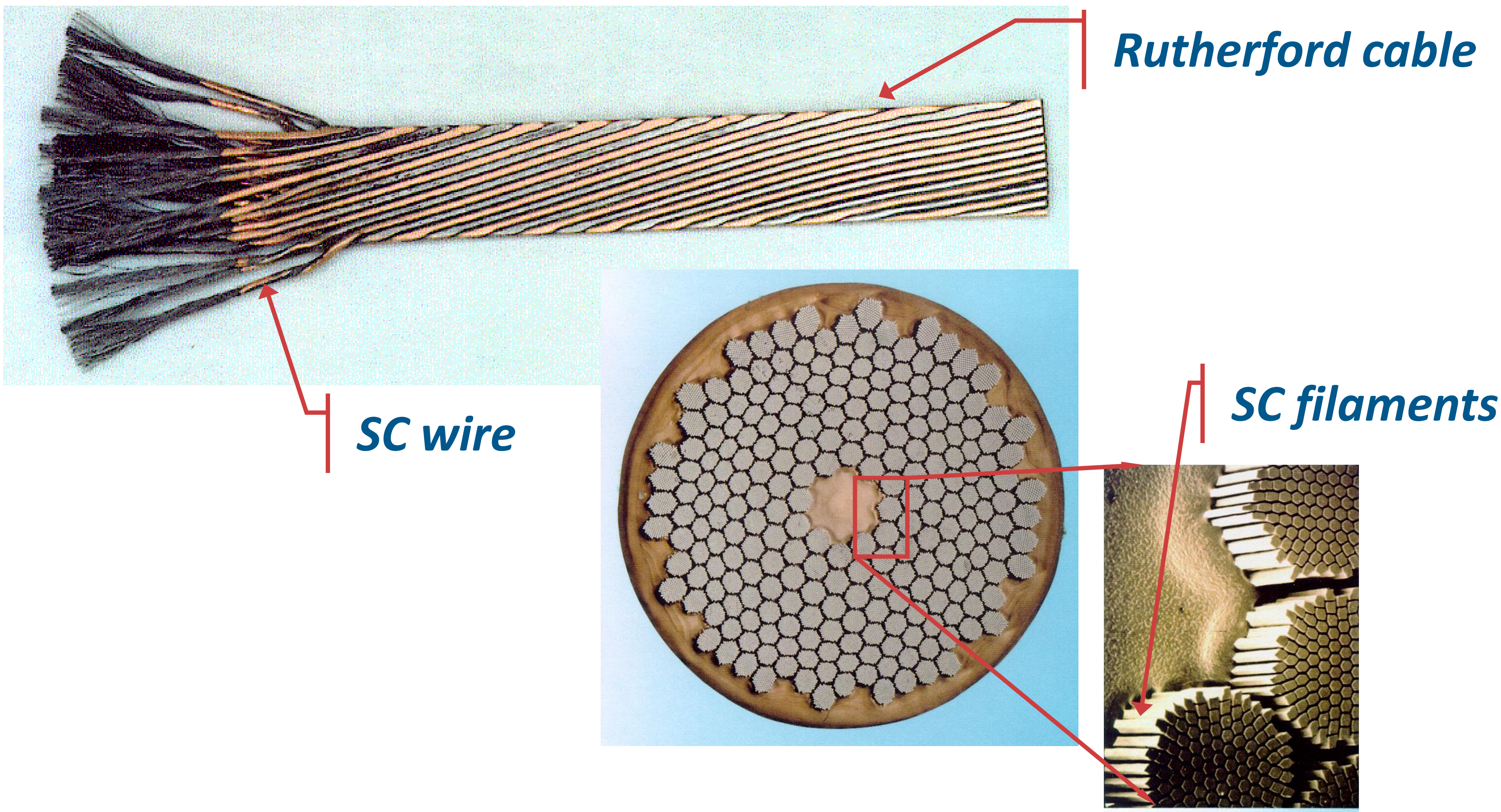

How to make the dipole able to sustain the stress

- *Clamping the winding in a solid collar*

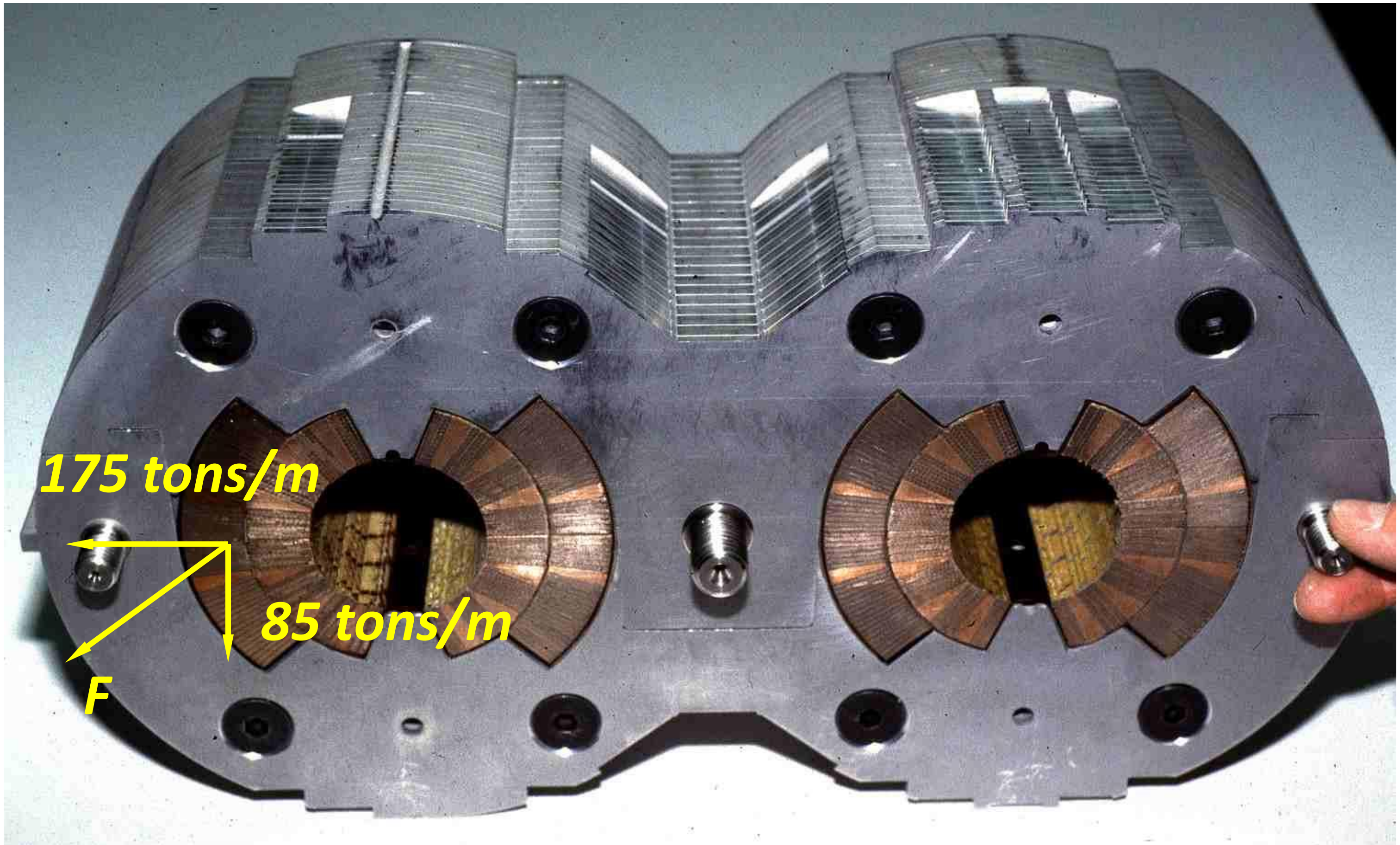

Magnetic forces in the ITER TF coils

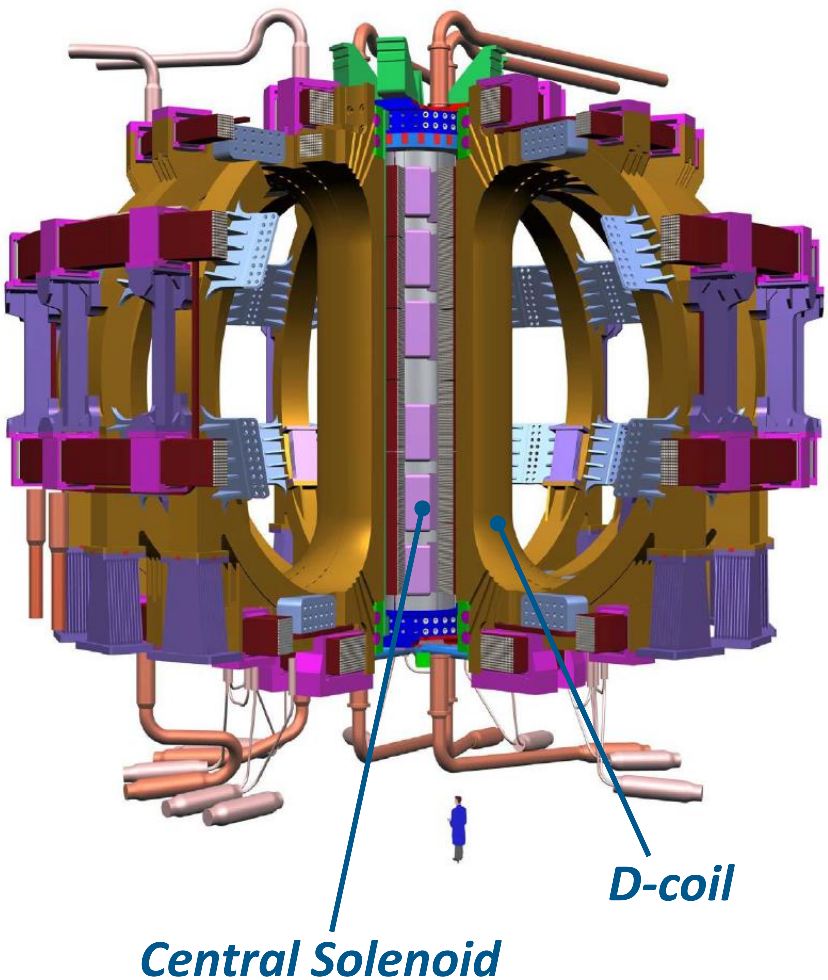

in-plane forces

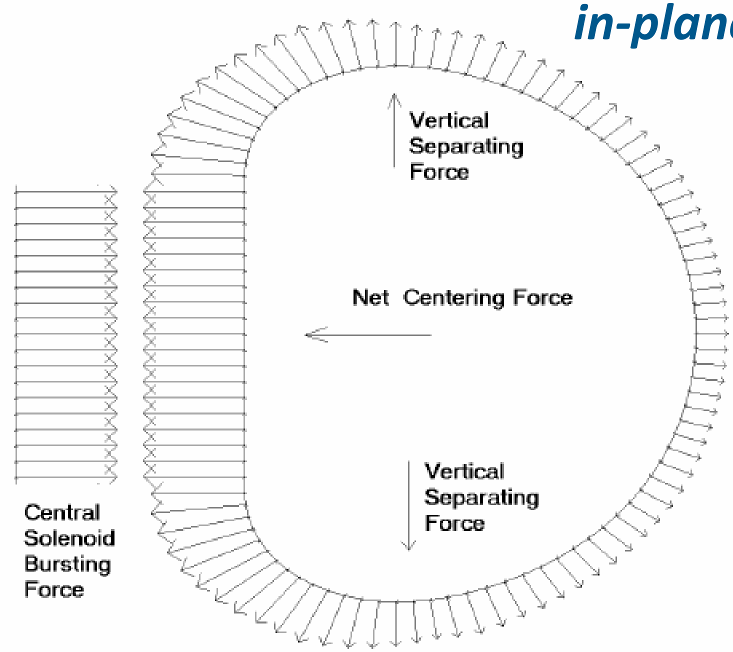

out-of-plane forces

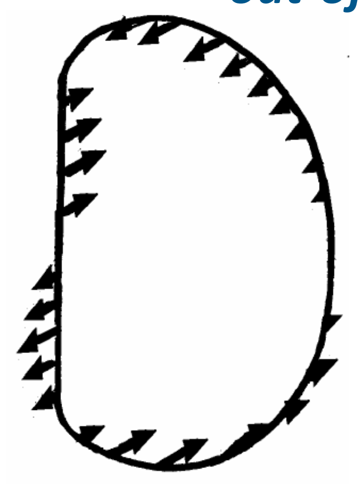

Wire cabling for the ITER coils

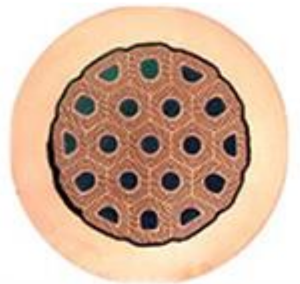

CICC = Cable-In-Conduit Conductor

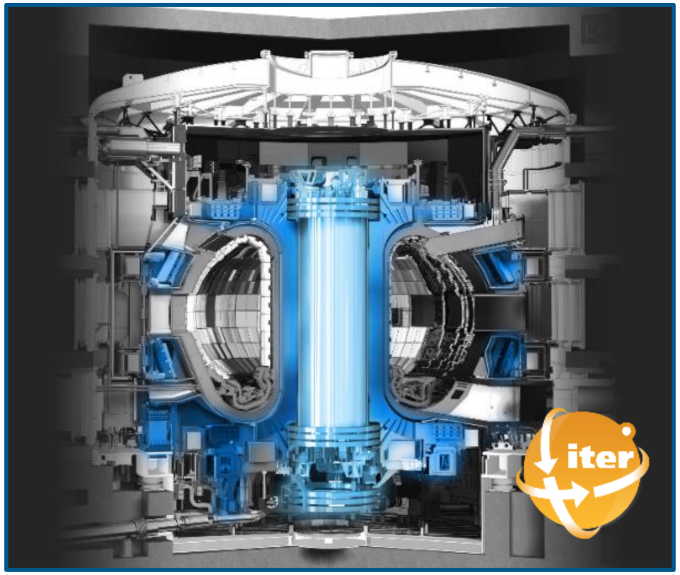

Thermal precompression of the superconductor

All technical superconductors are composite

Mismatch in thermal contraction within the composite induces a precompression in the SC

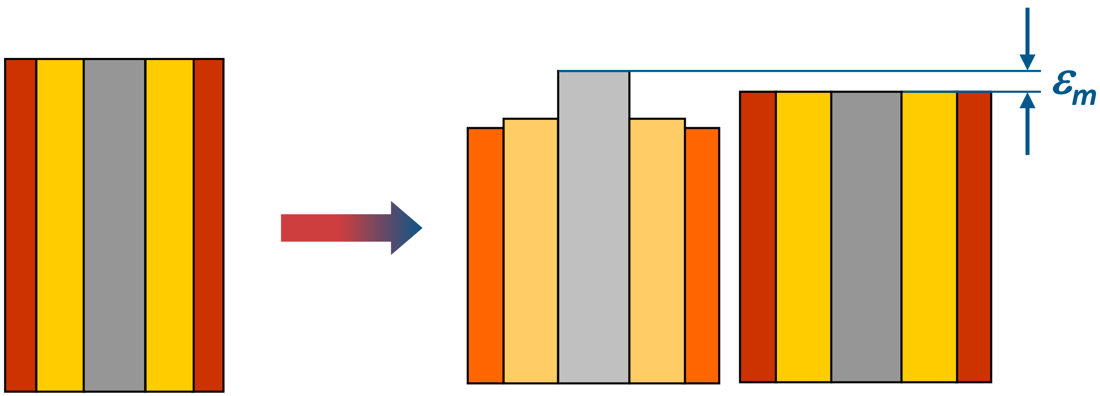

650°C ***4.2 K***

When the SC is cooled at the operating temperature, its crystal structure deforms and this induces changes on T_c , B_{c2} (and thus on J_c)

NbTi

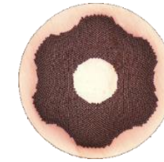

Nb_3Sn

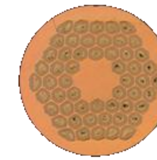

MgB_2

Bi2223

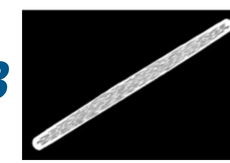

Bi2212

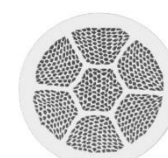

YBCO

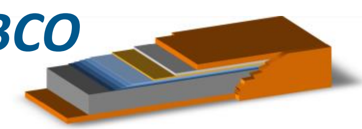

Strain-induced changes in the critical current

Effects of the longitudinal strain

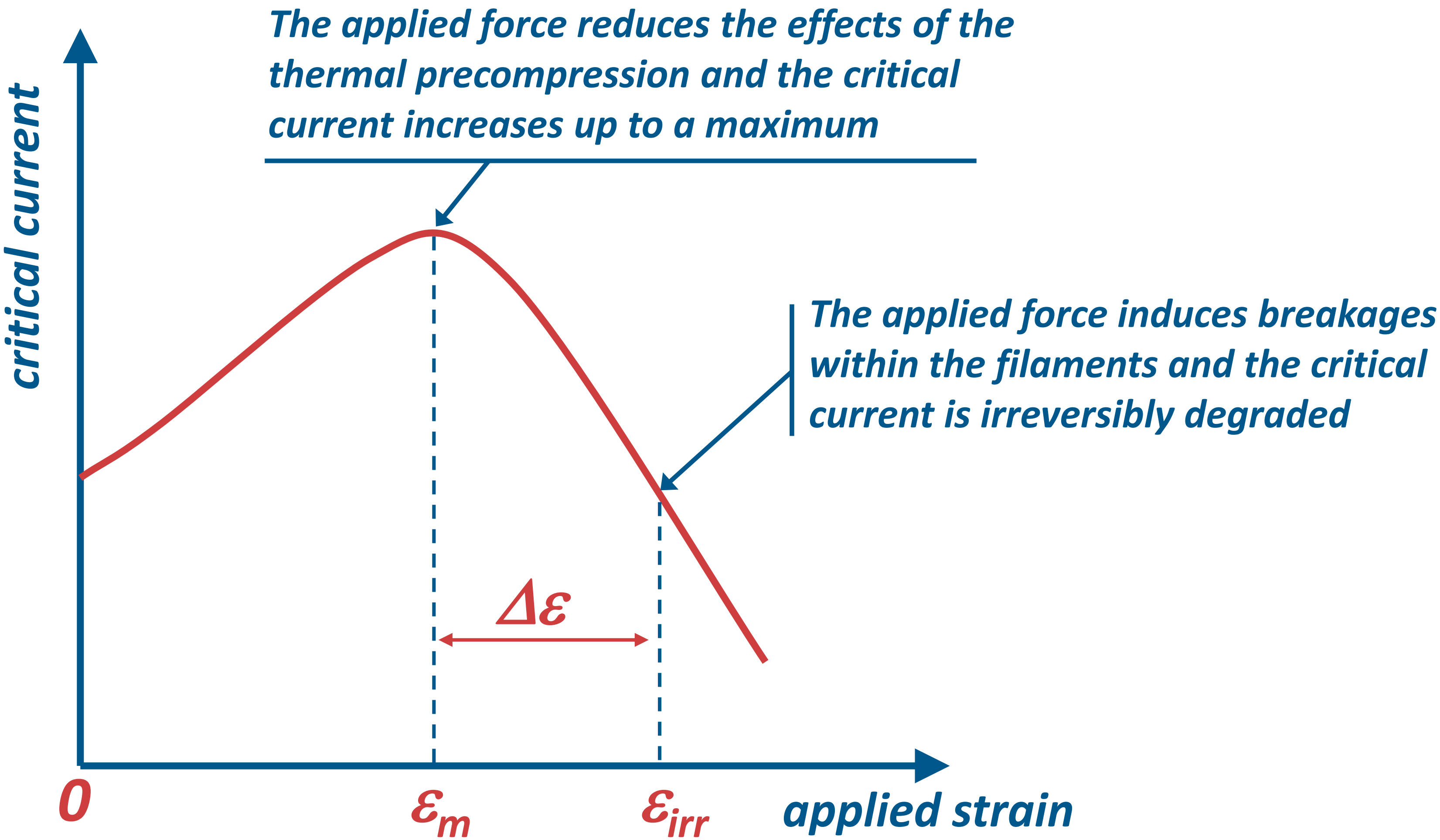

Strain-induced changes in the critical current

Effects of the longitudinal strain

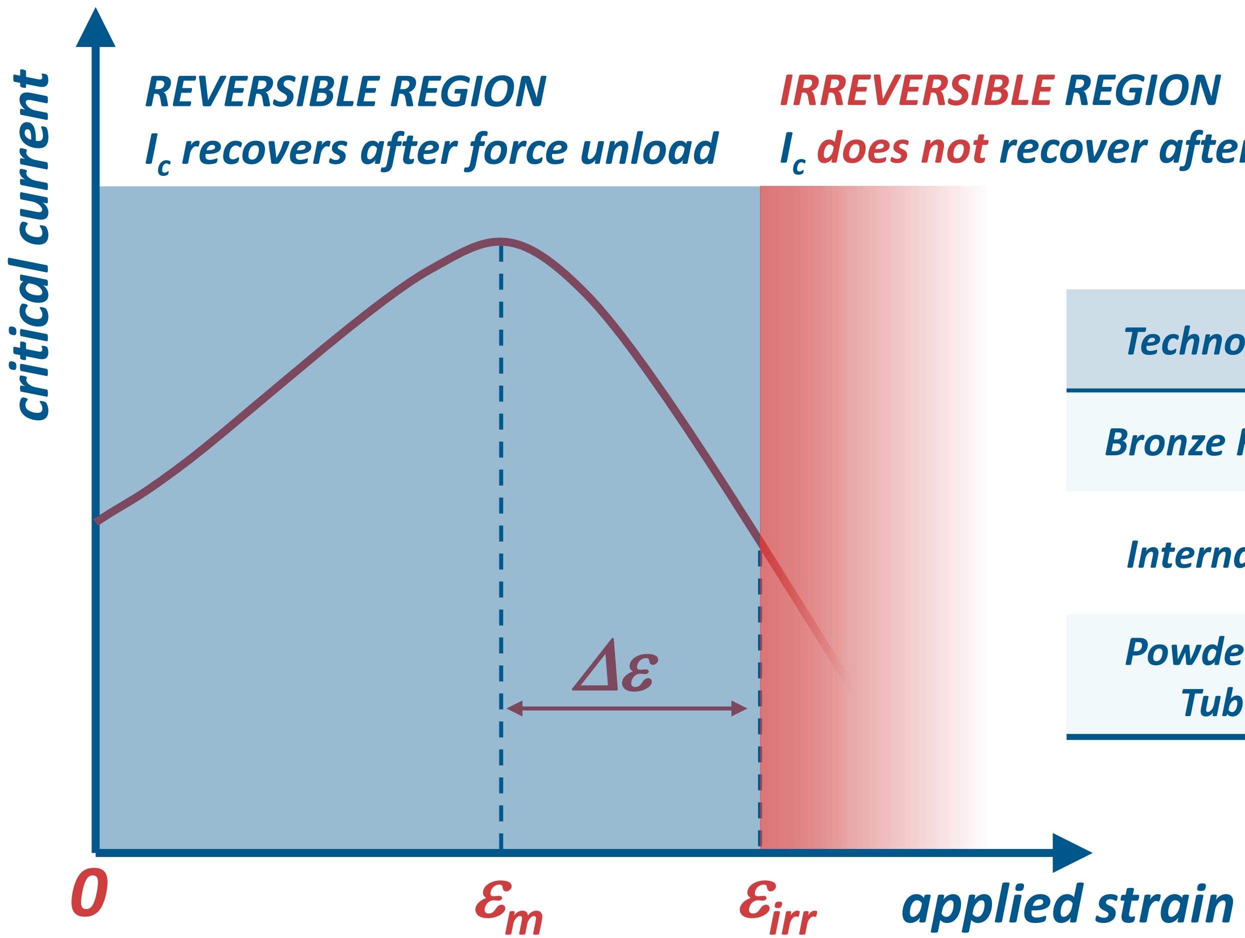

Technology	$\Delta\varepsilon = \varepsilon_m - \varepsilon_{irr}$ [%]
Bronze Route	0.4 – 0.6
Internal Sn	0.05 – 0.2
Powder-In-Tube	0.15 – 0.3

Wire cabling for the ITER coils

Reversible variation of I_c under strain matters

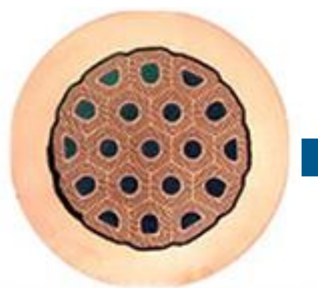

CICC = Cable-In-Conduit Conductor

Because of the thermal precompression, wires in a CICC experience an effective axial compressive strain ranging between -0.6% and -0.8%

The performance of the superconductor is limited to ~40% of the maximum achievable current

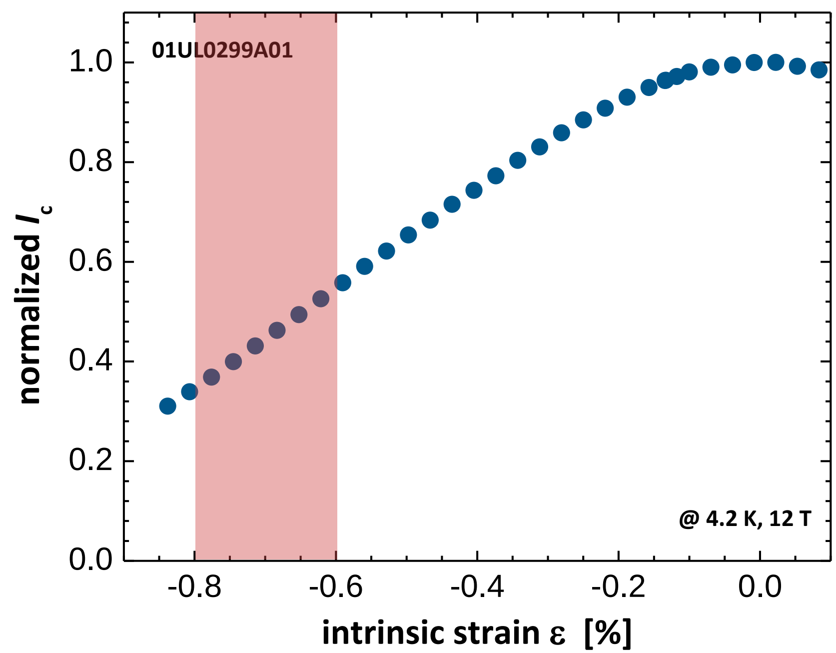

Reversible strain effects

Why superconducting properties depend on strain

Under strain the crystal structure deforms and this induces change both in the phonon spectrum and the electronic bands and thus on T_c and B_{c2}

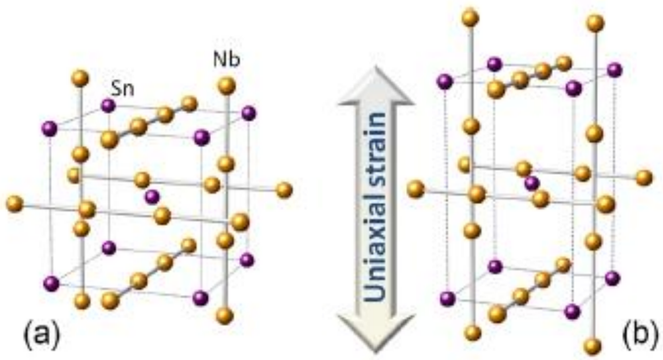

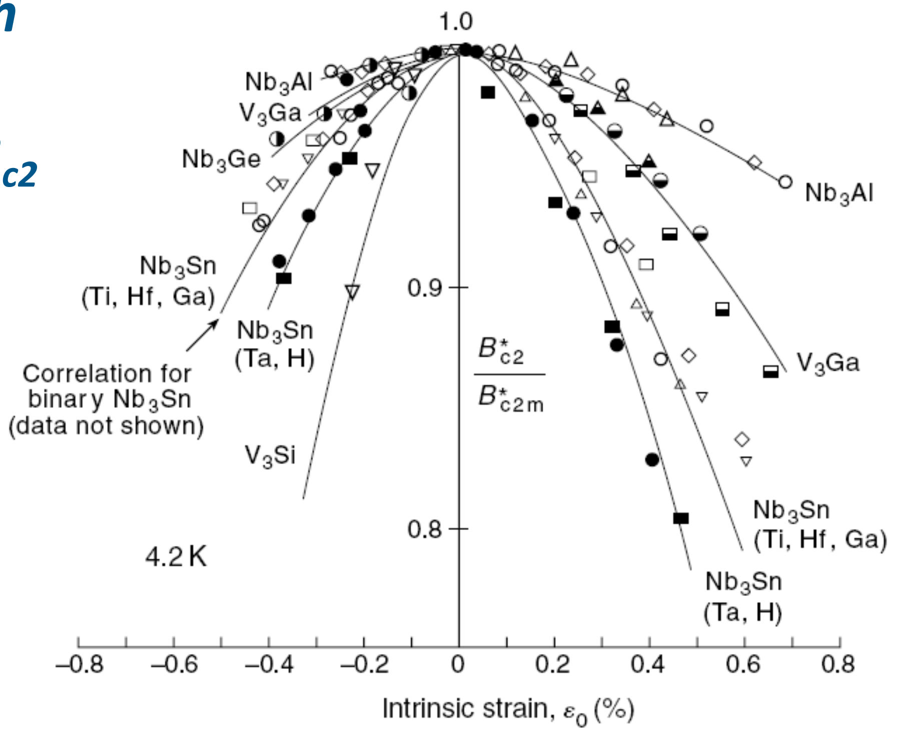

Reversible strain effects in Nb_3Sn wires

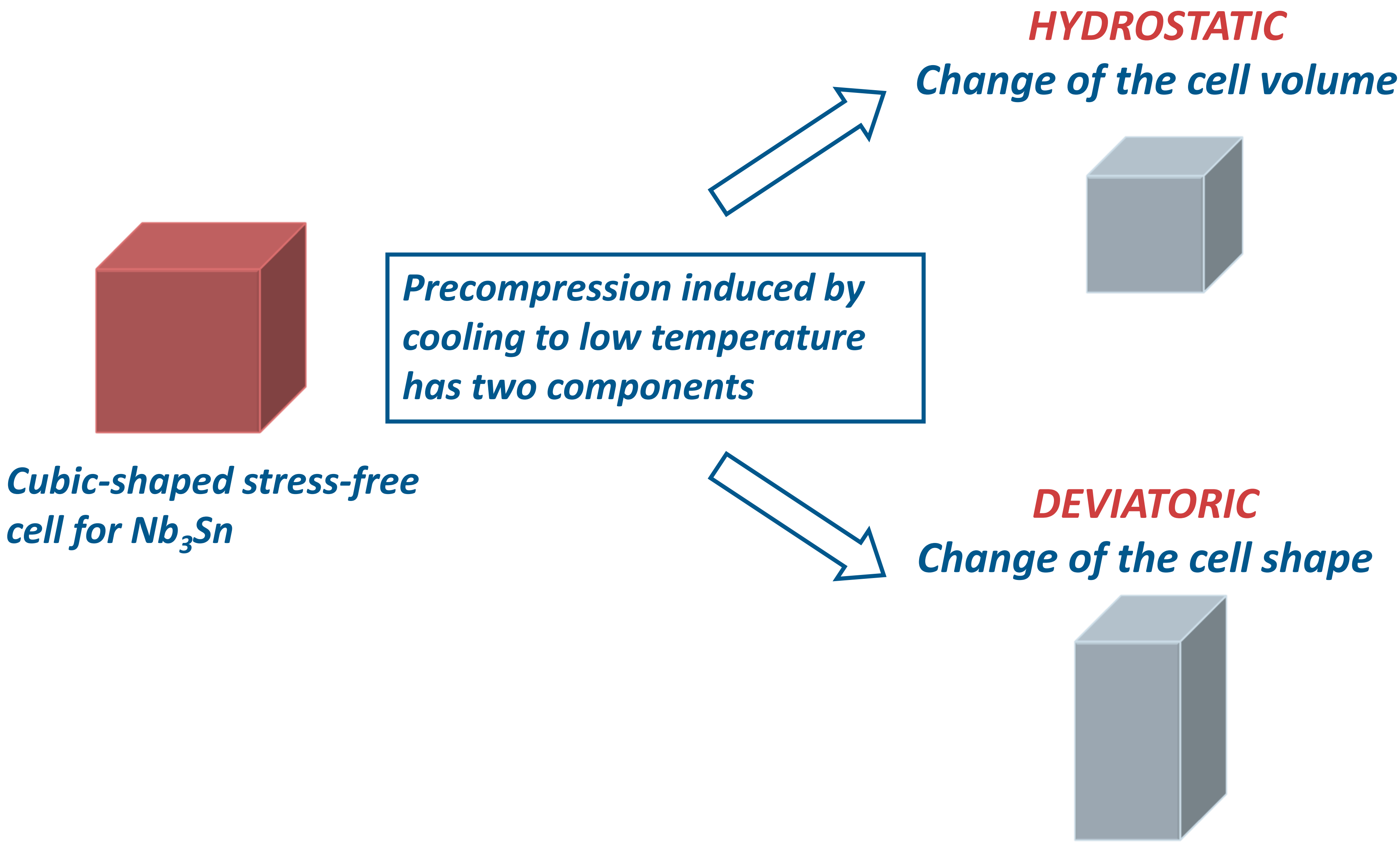

Reversible strain effects in Nb_3Sn wires: lattice parameters

Bronze route wire: Nb_3Sn lattice parameters vs uniaxial strain @ 4.2 K

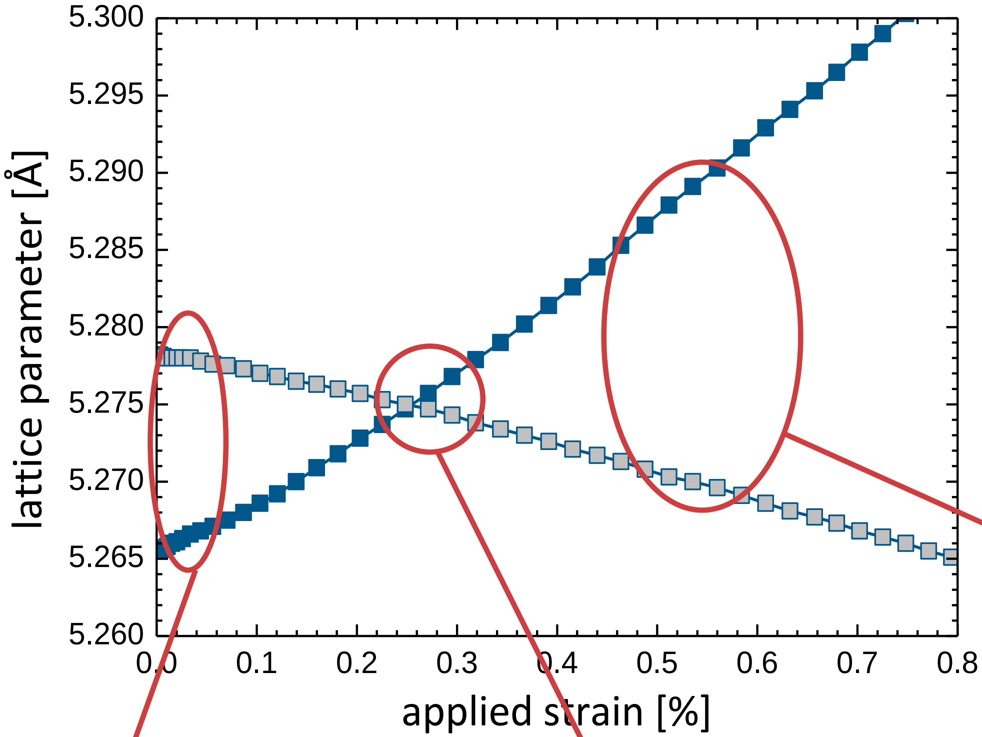

XRD experiments @ ESRF Grenoble

C. Scheuerlein et al., IEEE TAS 19 (2009) 2653

L. Muzzi et al., SUST 25 (2012) 054006

HIGH APPLIED STRAIN
Again Hydrostatic+Deviatoric

ZERO APPLIED STRAIN
Nb_3Sn is precompressed
Hydrostatic+Deviatoric

CROSSING POINT
Cubic cell recovered
Hydrostatic component still present

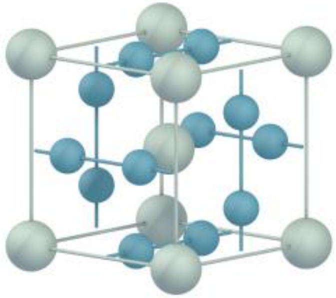

Lattice parameters and I_c under axial strain

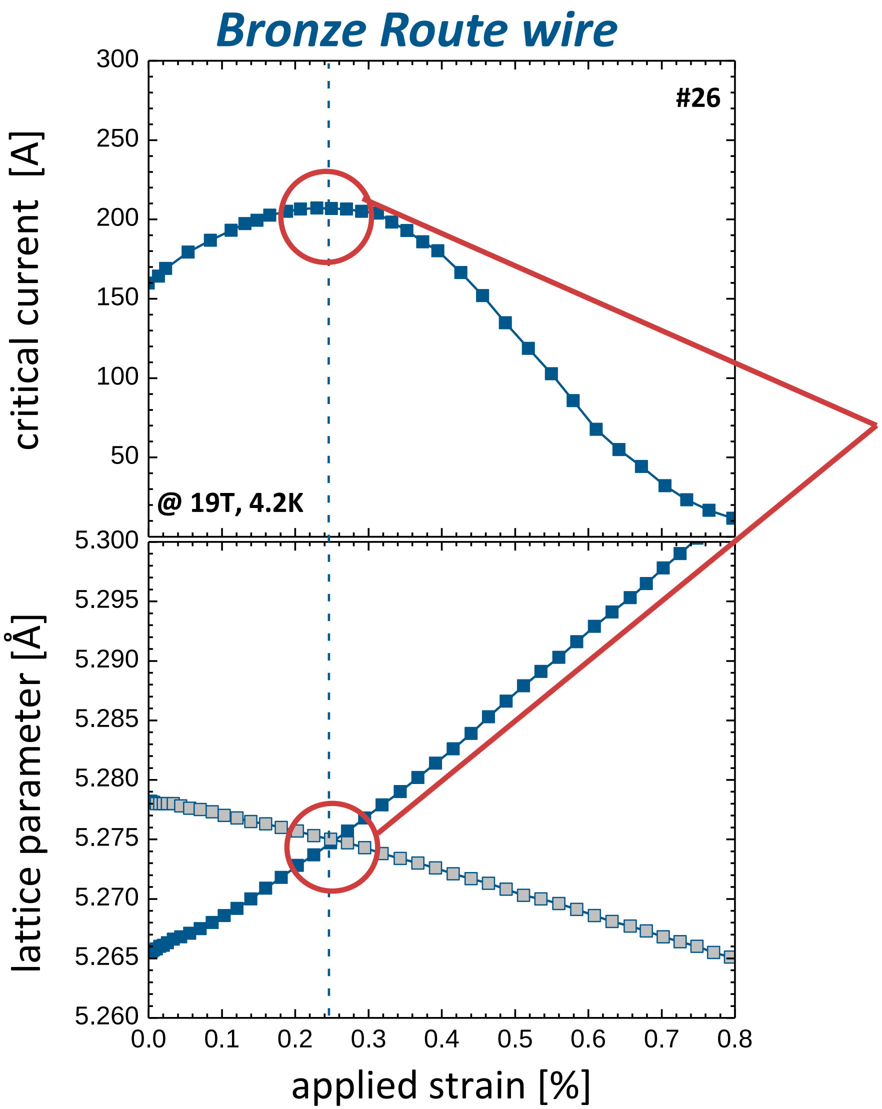

MAXIMUM OF I_c

The maximum of the critical current occurs when the cubic cell is restored

Bibliography

Wilson
Superconducting Magnets
Chapter 3
Chapter 4

Iwasa
Case Studies in Superconducting Magnets
Chapter 3 Section 3

Ekin
Experimental Techniques for Low-Temperature Measurements
Chapter 10 Section 5

Papers cited in the slides